ENERGY FUNCTIONS, TRANSIENT STABILITY AND VOLTAGE BEHAVIOUR IN POWER SYSTEMS WITH NONLINEAR LOADS

Ian A. Hiskens*, Member, IEEE David J. Hill, Member, IEEE

Department of Electrical and Computer Engineering
University of Newcastle
N.S.W. 2308, Australia.

ABSTRACT

This paper presents preliminary results in a program aimed at energy function analysis of transient behaviour of power systems with nonlinear loads. The model, which preserves the network structure, is of differential-algebraic type. This introduces some new analytical issues, but the concepts enable the establishment of a connection between transient (angle) stability, multiple stable equilibria and voltage behaviour. A practical method for determining and classifying equilibrium points of the model is developed.

I INTRODUCTION

Direct methods of determining power system transient stability using energy functions have been evolving for a number of years. Recently however, they have reached the stage where industry is starting to accept them as valid analysis tools capable of giving sufficiently accurate results for realistic power systems [1,2]. Through this interaction with industry, practical modelling and implementation difficulties are being identified.

A number of the major limitations experienced to date relate to the reduced network model (RNM) of the power system traditionally used as the basis of energy function methods. In this model, all loads are converted to constant admittances. Then the network is reduced to the generator internal buses [3]. Some concomitant problems are:

- Network sparsity is lost. By not maintaining sparsity, solution efficiency is reduced and solution time is increased. For large power systems this increase is significant. It has also been noted that for very large power systems, solution of the reduced network may not be possible at all, see comments by Tinney [4].
- Nonlinear loads cannot be modelled. The importance of correct load modelling is now widely recognized in utilities. Constant impedance load models often lead to optimistic assessment of system stability when compared to cases with significant constant power or constant current components [5].

*On leave from Queensland Electricity Commission, Australia.

89 WM 152-0 PWRS A paper recommended and approved by the IEEE Power System Engineering Committee of the IEEE Power Engineering Society for presentation at the IEEE/PES 1989 Winter Meeting, New York, New York, January 29 - February 3, 1989. Manuscript submitted August 25, 1988; made available for printing January 16, 1989.

These limitations can be overcome by the use of structure preserving models (SPM) of power systems; see discussions in [6,7]. As the name suggests, these models leave the structure (or topology) of the network in its original form. Therefore normal sparsity programming can be employed in the implementation of algorithms. Also, because the structure remains intact, complete with load buses, nonlinear load models can be easily incorporated. More accurate transient stability assessment results. Whereas considerable effort has gone into improving energy function methods with respect to generator modelling, computational experience suggests that the network model is typically more important to the essential transient stability problem.

Following the initial idea by Bergen and Hill [6], work on SPMs has progressed to develop better energy functions and show that some familiar techniques from studies with traditional RNMs can be used (namely PEBS type methods) [8-15]. However, it remains to exploit the potential of SPMs for large realistic systems. Further there are some interesting network cutset concepts which appear useful [6,16]. These connect closely with the demand in industry to relate stability assessment to familiar practical notions of 'weak boundaries' [17]. With these aims in sight it becomes clear that a deeper understanding is needed of SPMs and their energy functions. In mathematical terms, how the equilibria and energy functions are defined on manifolds associated with the model.

Perhaps the most important side issue in consideration of SPMs for transient stability analysis is voltage stability. Because explicit load models and network structure are incorporated in the SPM, many of the important elements of the voltage stability phenomena are modelled. It is clear that network voltage behaviour in the transient period is important to analysis of transient stability (large disturbance angle stability). There are numerous views on the problem of voltage collapse. The work which seems most relevant here relates to multiple solutions in load flow [18,19]. These solutions are the equilibria in dynamic SPMs.

The aim of this paper is to present results in progress towards a thorough study of the above ideas. It provides a basis for development of a direct transient stability assessment algorithm based on nonlinear loads, sparsity and weak cutsets. This algorithm is to be described separately. The emphasis here is on understanding the concepts and tools to be used. Throughout the paper, concepts are illustrated by reference to the four bus power system of Fig. 1. Many more details including proofs of some theoretical statements are omitted and can be found in the report [20].

II STRUCTURE PRESERVING MODELS

2.1 Model Development

The classical machine model is used in the development of this SPM. Therefore the synchronous machines are represented by a constant voltage $|E_i|$ in series with transient reactance. Other generator/exciter models could be substituted if necessary using established techniques [10,13,21]. However, in the present paper, this machine model simplifies the details of the

SPM and energy function without detracting from the main concepts.

Consider now a network consisting of n_o buses connected by transmission lines. At m of these buses there are generators. The buses which have load but no generation are labelled $i=1,\ldots,n_o-m$. The network is augmented with m fictitious buses representing the generator internal buses, in accordance with the classical machine model. They are labelled i+m where i is the bus number of the corresponding generator bus. The total number of buses in the augmented system is therefore $n_o+m:=n$.

The network is assumed lossless, so all lines (including those corresponding to the machine transient reactances) are modelled as series reactances. The bus admittance matrix $\underline{Y}$ is therefore purely imaginary, with elements $Y_{ij}=jB_{ij}$.

Let the complex voltage at the ith bus be the (time varying) phasor $V_i=|V_i|\angle\delta_i$ where δ_i is the bus phase angle with respect to a synchronously rotating reference frame. Define $|\underline{V}|=[|V_1|,\ldots,|V_{n_o}|]^t$, where 't' denotes matrix transpose. The bus frequency deviation is given by $\omega_i=\dot{\delta}_i$.

The SPM of interest is based on machine reference angles, with the nth bus taken as the reference. We use the internodal angles $\alpha_i:=\delta_i-\delta_n$. Define $\underline{\alpha}=[\alpha_1,\ldots,\alpha_{n-1}]^t$ and $\underline{\omega}_g=[\omega_{n_o+1},\ldots,\omega_n]^t$.

Let P_{bi} and Q_{bi} denote the total real and reactive power leaving the ith bus via transmission lines. Then

$$P_{bi}(\underline{\alpha},|\underline{V}|) = \sum_{j=1}^{n} |V_i||V_j|B_{ij}\sin(\alpha_i-\alpha_j) \qquad (1a)$$

$$Q_{bi}(\underline{\alpha},|\underline{V}|) = -\sum_{j=1}^{n} |V_i||V_j|B_{ij}\cos(\alpha_i-\alpha_j) \qquad (1b)$$

In these equations, we assume the substitution $|V_i|=|E_{i-n_o}|, i=n_o+1,\ldots,n$ has been made. Also we take $\alpha_n:=0$.

Now consider the modelling of loads. Denote the real and reactive power demand at the ith bus by P_{di} and Q_{di} respectively. In general these powers are functions of voltage and frequency. The loads shall be assumed to satisfy

$$P_{di} = P_{di}(|V_i|) \quad ; \quad i=1,\ldots,n_o \qquad (2a)$$

$$Q_{di} = Q_{di}(|V_i|) \qquad (2b)$$

In [15,20], it is shown that combining (1), (2) and the usual generator swing equations gives the model

$$\dot{\underline{\omega}}_g = -\underline{M}_g^{-1}\underline{D}_g\underline{\omega}_g-\underline{M}_g^{-1}\underline{T}_g^t(\underline{P}_g(\underline{\alpha}_g,\underline{\alpha}_\ell,|\underline{V}|)-\tilde{\underline{P}}_M^0) \qquad (3a)$$

$$\dot{\underline{\alpha}}_g = \underline{T}_g\underline{\omega}_g \qquad (3b)$$

$$\underline{0} = \underline{P}_\ell(\underline{\alpha}_g,\underline{\alpha}_\ell,|\underline{V}|)+\underline{P}_d(|\underline{V}|) := \underline{f}_\ell(\underline{\alpha}_g,\underline{\alpha}_\ell,|\underline{V}|) \qquad (4a)$$

$$\underline{0} = [|\underline{V}|]^{-1}(\underline{Q}_b(\underline{\alpha}_g,\underline{\alpha}_\ell,|\underline{V}|)+\underline{Q}_d(|\underline{V}|)) := \underline{g}(\underline{\alpha}_g,\underline{\alpha}_\ell,|\underline{V}|) \qquad (4b)$$

$\underline{M}_g$, $\underline{D}_g$ are diagonal matrices of inertia, damping constants. The angle vector $\underline{\alpha}$ is partitioned as $\underline{\alpha}^t=[\underline{\alpha}_\ell^t\ \underline{\alpha}_g^t]$. Subscripts ℓ,g will be used to denote loads, generators respectively. $\tilde{\underline{P}}_M^0$ is the (m-1)-vector of mechanical powers excluding reference machine. (Some transformation of powers is often required to achieve the precise form (3) [22].) $\underline{T}_g$ is a specially structured matrix of ±1 entries and $[\underline{a}]$ denotes $[\mathrm{diag}\{a_i\}]$ for vector $\underline{a}$.

Equations (3), (4) describe the model denoted SPM_o, which all further results are based upon. Note that it consists of a set of differential-algebraic equations. The system variables are clearly $\underline{\omega}_g \in \mathbb{R}^m$, $\underline{\alpha}_g \in \mathbb{R}^{m-1}$, $\underline{\alpha}_\ell \in \mathbb{R}^{n_o}$, and $|\underline{V}| \in \mathbb{R}_+^{n_o}$.

2.2 Local ODE Representation of SPM_o

Differential-algebraic equations of the form (3), (4) are theoretically problematic [23]. Fortunately, here it can be shown that the model is locally equivalent to a set of ordinary differential equations for almost all operating states. The load bus variables $\underline{\alpha}_\ell$, $|\underline{V}|$ are related to the generator angles $\underline{\alpha}_g$ by the $2n_o$ algebraic equations (4). In fact, (4) defines an (m-1)-manifold on which $\underline{\alpha}_g$ can flow. Define the Jacobian

$$\underline{J}_{\ell\ell} = \begin{bmatrix} \dfrac{\partial \underline{f}_\ell}{\partial \underline{\alpha}_\ell} & \dfrac{\partial \underline{f}_\ell}{\partial |\underline{V}|} \\ \dfrac{\partial \underline{g}}{\partial \underline{\alpha}_\ell} & \dfrac{\partial \underline{g}}{\partial |\underline{V}|} \end{bmatrix} \qquad (5)$$

Then, by the implicit function theorem [24], if $\det \underline{J}_{\ell\ell}\neq 0$, locally the load bus variables can be written explicitly in terms of the generator angles as

$$\underline{\alpha}_\ell = \Phi(\underline{\alpha}_g) \quad , \quad |\underline{V}| = \Psi(\underline{\alpha}_g) \qquad (6)$$

An equivalent differential equation form of the SPM_o can therefore be obtained locally by substituting (6) into (3a). Setting $\underline{P}_g^*(\underline{\alpha}_g) := \underline{P}_g(\underline{\alpha}_g,\Phi(\underline{\alpha}_g),\Psi(\underline{\alpha}_g))$ gives the model

$$\dot{\underline{\omega}}_g = -\underline{M}_g^{-1}\underline{D}_g\underline{\omega}_g-\underline{M}_g^{-1}\underline{T}_g^t(\underline{P}_g^*(\underline{\alpha}_g)-\tilde{\underline{P}}_M^0) \qquad (7a)$$

$$\dot{\underline{\alpha}}_g = \underline{T}_g\underline{\omega}_g \qquad (7b)$$

Equations (7) define ordinary differential equations which are locally equivalent to SPM_o.

This idea of local solvability can be extended to solvability over disjoint regions via the following theorem.

Theorem 1. Suppose that for the non-empty compact set C_ℓ $\det \underline{J}_{\ell\ell}|(\underline{\alpha}_g,\underline{\alpha}_\ell,|\underline{V}|) \in C_\ell \neq 0$; and $\underline{J}_{\ell\ell}|(\underline{\alpha}_g,\underline{\alpha}_\ell,|\underline{V}|) \in C_\ell$ has ℓ negative eigenvalues. Let $A_\ell=\{\underline{\alpha}_g:(\underline{\alpha}_g,\underline{\alpha}_\ell,|\underline{V}|) \in C_\ell\}$. Then there exist unique continuous functions $\Phi_\ell:A_\ell\to\mathbb{R}^{n_o}$, $\Psi_\ell:A_\ell\to\mathbb{R}^{n_o}$ such that over C_ℓ SPM_o can be written in the form (7).

Comments:

1. As $\underline{J}_{\ell\ell}$ has dimension $2n_o$, ℓ can take the values

$0,\ldots,2n_o$. Therefore the maximum number of sets C_ℓ which can exist for SPM_o is $2n_o+1$.
2. The sizes of sets C_ℓ depend of course on the load model parameters. Conditions are given in Appendix A for ensuring C_ℓ, $\ell\neq 0$, are empty. However, these are not always satisfied in practice [25].

2.3 Forms of Stability for SPM_o

1. Angle stability. This is the traditional concept of power system transient stability. It is the stability of the model (7), i.e. the ability of $\underline{\alpha}_g$ to settle to a post-disturbance stable EP.
2. Voltage causality. This is the requirement that the load bus voltages and angles always behave in a manner dependent on the generator angles. Voltage causality is guaranteed over the sets C_ℓ defined above. Henceforth, we refer to sets C_ℓ as voltage causal regions. On the surface $\det \underline{J}_{\ell\ell}=0$, $\underline{\alpha}_\ell$ and $|\underline{V}|$ are no longer dependent on $\underline{\alpha}_g$. The model breaks down and voltage behaviour can no longer be predicted. This surface shall be referred to as the "impasse" surface, using terminology from circuit theory [29]. (Lack of voltage causality can sometimes be observed when a trajectory of SPM_o is being obtained by numerical integration. As the trajectory encounters the impasse surface, the integration technique will fail to converge.)

This terminology certainly does not aim to cover the phenomenon of long-term voltage collapse where other aspects of the system should be modelled and added to SPM_o. We are only concerned with the short-term behaviour.

III DETERMINATION OF SYSTEM EQUILIBRIA

3.1 Conceptual Background

An intuitive approach to finding EPs is to view the equilibrium equations of SPM_o as defining the (m-1)-manifold which would result if $\tilde{\underline{P}}^0_M$ were allowed to vary. All EPs for a given $\tilde{\underline{P}}^0_M$ must lie on the manifold. If one element of $\tilde{\underline{P}}^0_M$ is then constrained to its actual value, a slice is taken through the (m-1)-manifold, so an (m-2)- manifold results. On this manifold lie the solutions of the equilibrium equations which would result if all elements of $\tilde{\underline{P}}^0_M$ except one were allowed to vary. Again, all EPs must lie on this manifold.

This process of slicing through the manifold by successively enforcing $\tilde{\underline{P}}^0_M$ constraints is continued until a 1-manifold or curve remains. Following the same argument, all EPs must lie on this 1-manifold. One last slice through this 1-manifold by constraining the last element of $\tilde{\underline{P}}^0_M$ gives all the EPs. This last slice is simply the intersections of a curve and a straight line. Clearly, this curve can be presented on a plane as a relation between the last P^0_{Mi}, and any other variable of interest.

3.2 An Efficient EP Search Routine

Whilst the concept behind the algorithm is to start from the most general space and continually constrain the solution, the actual algorithm works in reverse. Starting from a known EP, one element of $\tilde{\underline{P}}^0_M$ is released. A 1-manifold results. Points on this curve are obtained using CONTUR, a program developed by Price [26]. Sucessive points on the curve are calculated until the power at the generator bus corresponding to the released constraint again equals its initial value. An EP of the system has been found. CONTUR can find all EPs by continuing to track around the 1-manifold. The 1-manifold is observed to be closed, so the procedure is halted when the starting point is encountered.

Comments

1. The complete description of each EP obtained in this way is part of the CONTUR output [26].
2. In general real power loads are voltage dependent. Around the 1-manifold, voltages are varying, so loads must also vary. In this case only the initial (i.e. known) EP corresponds to the generator power constraints $\tilde{\underline{P}}^0_M$. At other EPs, generator powers are transformed [15]. This transformation is easily implemented into the algorithm by allowing the slack at the reference generator to be distributed across all constrained generators. Constraining the remaining transformed generator power determines the EPs.

Example

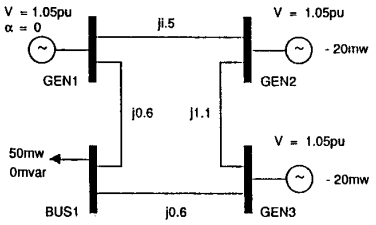

Fig.1: One Line Diagram of 4-Bus System.

Consider the small power system of Fig. 1. This system consists of three generator buses and one load bus. (It does not meet the numbering convention of Section 2.1, but usefully illustrates all the concepts which will be encountered.) The load is taken to be of constant power type. This is deliberately chosen to not satisfy the conditions of Appendix A. Thus we expect multiple sets C_ℓ. By releasing the real power constraint at generator 2, the 1-manifold of Fig. 2 results. It is plotted with reference to MVAR at generator 2 to show the large differences in reactive power requirements between EPs. The original GEN2 power was -0.2pu, shown by line A-A in Fig. 2. This line intersects the 1-manifold at two points, 'a' and 'b', the only EPs of this system. Point 'a' was the original EP.

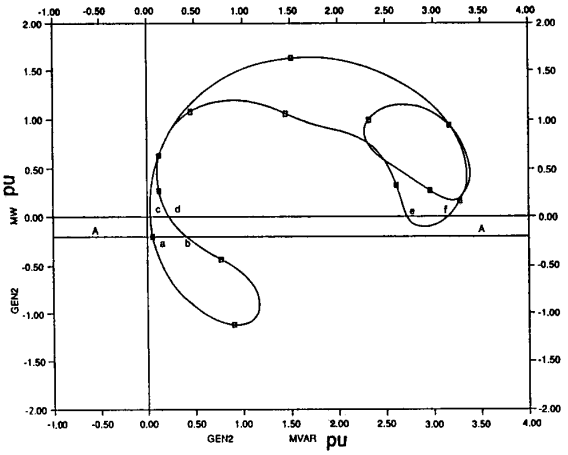

Fig.2: GEN2 1-Manifold.

Notice that if the initial GEN2 power was 0pu, the system would have four EPs given by the intersections of the x-axis and the 1-manifold. □

IV CLASSIFICATION OF EQUILIBRIUM POINTS

4.1 Linearized System Equations

$$\text{Let } \underline{f}_g := \underline{P}_g(\underline{\alpha}_g, \underline{\alpha}_\ell, |\underline{V}|) - \tilde{P}_M^0 \tag{8}$$

Then, linearizing SPM_o, (3), (4) gives

$$\Delta\dot{\underline{\omega}}_g = -\underline{M}_g^{-1}\underline{D}_g\Delta\underline{\omega}_g - \underline{M}_g^{-1}\underline{T}_g^t\Delta\underline{f}_g$$

$$\Delta\dot{\underline{\alpha}}_g = \underline{T}_g\Delta\underline{\omega}_g$$

and

$$\begin{bmatrix}\Delta\underline{f}_\ell = \underline{0}\\ \Delta\underline{g} = \underline{0}\\ \Delta\underline{f}_g\end{bmatrix} = \begin{bmatrix} & \vdots & \frac{\partial\underline{f}_\ell}{\partial\underline{\alpha}_g}\\ \underline{J}_{\ell\ell} & \vdots & \frac{\partial\underline{g}}{\partial\underline{\alpha}_g}\\ \cdots & \vdots & \cdots\\ \frac{\partial\underline{f}_g}{\partial\underline{\alpha}_\ell} \quad \frac{\partial\underline{f}_g}{\partial|\underline{V}|} & \vdots & \frac{\partial\underline{f}_g}{\partial\underline{\alpha}_g}\end{bmatrix}\begin{bmatrix}\Delta\underline{\alpha}_\ell\\ \Delta|\underline{V}|\\ \Delta\underline{\alpha}_g\end{bmatrix} \tag{9}$$

Solving for $\Delta\underline{f}_g$ in (9), and substituting yields the linearized version of SPM_o as

$$\begin{bmatrix}\Delta\dot{\underline{\alpha}}_g\\ \Delta\dot{\underline{\omega}}_g\end{bmatrix} = \begin{bmatrix}0 & \vdots & \underline{T}_g\\ \cdots & \vdots & \cdots\\ -\underline{M}_g^{-1}\underline{T}_g^t\underline{F} & \vdots & -\underline{M}_g^{-1}\underline{D}_g\end{bmatrix}\begin{bmatrix}\Delta\underline{\alpha}_g\\ \Delta\underline{\omega}_g\end{bmatrix} = \underline{A}\begin{bmatrix}\Delta\underline{\alpha}_g\\ \Delta\underline{\omega}_g\end{bmatrix} \tag{10}$$

where

$$\underline{F} = \frac{\partial\underline{f}_g}{\partial\underline{\alpha}_g} - \begin{bmatrix}\frac{\partial\underline{f}_g}{\partial\underline{\alpha}_\ell} & \frac{\partial\underline{f}_g}{\partial|\underline{V}|}\end{bmatrix}\underline{J}_{\ell\ell}^{-1}\begin{bmatrix}\frac{\partial\underline{f}_\ell}{\partial\underline{\alpha}_g}\\ \frac{\partial\underline{g}}{\partial\underline{\alpha}_g}\end{bmatrix} \tag{11}$$

Comments

1. This system is stable (angle-wise) if and only if all eigenvalues of $\underline{A}$ have negative real parts.
2. If det $\underline{J}_{\ell\ell}=0$, this linearized model breaks down. This is the same condition as caused lack of voltage causality in SPM_o. As in the case of SPM_o, this model breakdown is a direct consequence of the load bus variables (in this case linearized) no longer being dependent on the generator angles (also linearized). This is seen by rearranging (9). If det $\underline{J}_{\ell\ell}=0$, no valid relationship exists between $\Delta\underline{\alpha}_\ell$, $\Delta|\underline{V}|$ and $\Delta\underline{\alpha}_g$.

4.2 Efficient Determination of EP Types

The process of building the system $\underline{A}$ matrix and then finding all its eigenvalues is computationally expensive. Actually we are not interested in the values of the eigenvalues, only in the signs of their real parts. Fortunately two results enable these signs and hence the EP type, to be determined without any extra computation at all.

Proposition 1 [20]: Suppose $\underline{S}$, a symmetric non-singular matrix, is factorized using normal Gaussian elimination as $\underline{S}=\underline{L}\underline{U}$ where $\underline{L}$ is lower unit triangular, and $\underline{U}$ is upper triangular. Then the number of negative diagonal elements of $\underline{U}$ is equal to the number of negative eigenvalues of $\underline{S}$.

Proposition 2 [27]: The number of positive eigenvalues of $\underline{A}$ is equal to the number of negative eigenvalues of $\underline{F}$.

If a Newton-based iterative technique is used to obtain the EP, as it is in CONTUR, the Jacobian (9) is available and factorized. Further, by ensuring it is ordered as in (9) with $\Delta\underline{f}_g$ last, after the first $2n_o$ rows and columns have been factorized, the $(m-1)\times(m-1)$ matrix remaining in the bottom right corner is $\underline{F}$, given by (11). Note that if det $\underline{J}_{\ell\ell}=0$, the factorization process will fail during these initial $2n_o$ steps, because of a divide by zero error.

Continuing the factorization process to completion, the last m-1 diagonals correspond to the factorized $\underline{F}$ matrix. By Proposition 1, the signs of the last m-1 diagonal elements of $\underline{U}$ correspond to the signs of the eigenvalues of $\underline{F}$, i.e. if ℓ of the last m-1 diagonals are negative, then $\underline{F}$ has ℓ negative eigenvalues. (Because $\underline{F}$ is symmetric its eigenvalues are real.) But, by Proposition 2, that means that $\underline{A}$ has ℓ eigenvalues with positive real parts. Therefore the EP is type-ℓ.

We have determined the EP type as a byproduct of solving for the EP.

Example (cont.)

We now return to the four bus example of Fig. 1. Classifying points 'a' and 'b' in the manner described above, it is found that they are both type-0 EPs, i.e. they are both small disturbance stable. Further investigation of these points shows that at 'a' all eigenvalues of $\underline{J}_{\ell\ell}$ are positive, whilst at 'b' one eigenvalue of $\underline{J}_{\ell\ell}$ is negative. This has no bearing on (angle) stability at all, but practical observation indicates that 'a' would be considered the 'normal' stable operating point of the power system.

Consider the EPs along the x-axis. They are classified as: 'c' is type-0, 'd' is type-0, 'e' is type-1, 'f' is type-2. At each of the points 'd', 'e', 'f', one eigenvalue of $\underline{J}_{\ell\ell}$ is negative. □

Comments

1. The issue of multiple solutions to load flow is important to discussions of voltage stability [18]. This example shows that care is needed in statements about voltage and/or angle stability of these solutions.
2. Whilst in general a negative eigenvalue of $\underline{J}_{\ell\ell}$ does not imply instability for SPM_o, if the system contains devices which are sensitive to $\frac{\partial g_i}{\partial|V_i|}$ or $\frac{\partial f_{\ell i}}{\partial\alpha_i}$, e.g., SVCs, then unstable behaviour may occur in the modelled extra states of those devices.

V LARGE DISTURBANCE ANALYSIS

In this section, we provide some basic methodology for determining large disturbance stability of the EPs. Emphasis is given to new insights on the nature of energy surfaces in the presence of multiple equilibria.

5.1 Energy Function

The development of energy functions for the model SPM_o has been studied elsewhere [9,15] using first integral and Lur'e problem analysis methods. A valid energy function is

$$V(\underline{\omega}_g,\underline{y}) = \frac{1}{2}\underline{\omega}_g^t\underline{M}_g\underline{\omega}_g + \int_{\underline{y}_S}^{\underline{y}} < \underline{h}(\underline{y}),d\underline{y} > \tag{12}$$

where $\underline{y}^t=[\underline{\alpha}_g^t\underline{\alpha}_\ell^t|\underline{V}|^t]$, $\underline{h}(\underline{y})^t=[\underline{f}_g(\underline{y})^t\underline{f}_\ell(\underline{y})^t\underline{g}(\underline{y})^t]$ and $\underline{y}_S$ denotes a stable EP. This function can be evaluated as

$$V(\underline{\omega}_g,\underline{\alpha}_g,\underline{\alpha}_\ell,|\underline{V}|) = \frac{1}{2}\underline{\omega}_g^t \underline{M}_g\underline{\omega}_g - \frac{1}{2}\sum_{i=1}^{n}\sum_{j=1}^{n} B_{ij}(|V_i||V_j|\cos\alpha_{ij} - |V_i^s||V_j^s|\cos\alpha_{ij}^s) - \int_{\underline{\alpha}^s}^{\underline{\alpha}} \tilde{\underline{P}}(|\underline{V}|)^t d\underline{\alpha} + \sum_{i=1}^{n_o}\int_{|V_i^s|}^{|V_i|}\frac{Qd_i(\mu_i)}{\mu_i}d\mu_i \qquad (13)$$

Comments

1. It can be shown that voltage dependence of Pd_i leads to similar analytical difficulties as transfer conductances in RNMs [8,15]. The integral $-\int_{\underline{\alpha}^s}^{\underline{\alpha}} \tilde{\underline{P}}(|\underline{V}|)^t d\underline{\alpha}$ becomes path dependent. The details of approximating this integral are similar to those for the path dependent integrals of non-zero transfer conductances.
2. In general the energy function V is multi-valued. This is inherited from the relation between $\underline{\alpha}_\ell, |\underline{V}|$ and $\underline{\alpha}_g$.
3. In [15] it is shown that a more general kinetic energy term can be used. Also if the damping $\underline{D}_g$ is zero or uniform [3], various refinements of this term are appropriate. The zero damping version is equivalent to a useful COA angle version [14].

5.2 Stability Results

The following result establishes the connection between small disturbance stability (Section 4) and asymptotic stability for EPs of SPM_o.

Theorem 2: If an equilibrium point $\underline{y}_e$ is "small disturbance stable" in the sense of Section 4.1, then it is asymptotically stable with respect to SPM_o.

The proof of this theorem is given in [20].

In Section 2.2, local solvability of (4) was extended to solvability over voltage causal regions. The same concept can be used to extend the region of validity of the local representation of V. In [20], theoretical estimates of the regions of attraction to stable EPs are given.

5.3 Multiple Energy Function Sheets

If the energy function (12) is treated in the usual way as the sum of kinetic and potential energy terms, then it is only the potential energy term which is dependent on the set C_ℓ. The local potential energy functions are functions of $\underline{\alpha}_g$ only, and so can be conceptualized as (m-1)-hypersurfaces (or sheets) in $\underline{\alpha}_g$-space. (Recall the potential energy well concept in [28].)

For each region C_ℓ defined by Theorem 1, a unique local potential energy function exists. By the comments made after that theorem, there could exist up to $2n_o+1$ such PE functions, each one a sheet in $\underline{\alpha}_g$-space. It is not difficult to imagine therefore how it is possible to have a number of asymptotically stable EPs. (Those sheets with a locally positive definite section must have an asymptotically stable EP at the lowest point of that section.) Note that not all sheets need contain an EP however.

All the PE sheets join on the impasse surface. To illustrate this, consider a point $\underline{y}_o$ on the manifold (4), where $\det \underline{J}_{\ell\ell}|_{\underline{y}_o}=0$, i.e., it lies on the impasse surface. $\underline{J}_{\ell\ell}|_{\underline{y}_o}$ must have at least one zero eigenvalue. Suppose it has just one zero eigenvalue, and ℓ negative eigenvalues. An infinitesimal movement of that point over the manifold, away from the impasse surface, will result in the zero eigenvalue becoming non-zero. If the eigenvalue goes positive, the point will become an element of C_ℓ, otherwise it will become an element of $C_{\ell+1}$. On each of these sets is a unique local PE sheet. Therefore, the sheets can be thought of as approaching each other infinitesimally closely at the impasse surface. Because this illustration is not dependent on ℓ, it follows that all sheets must approach each other at the impasse surface.

Given that the potential energy sheets lie one on top of the other, and are joined at the impasse surface, it seems reasonable to expect that the lowest sheet, which corresponds to C_o, must be deeper in terms of the potential energy well, than those stacked above it. Therefore the stable EP of C_o must have a larger stability margin than other stable EPs (if any exist). This is consistent with the fact that load bus voltages on the sets C_ℓ, $\ell\neq 0$, are depressed when compared with those on C_o. These depressed voltages reduce the power transfer capabilities, and hence stability margins, for the other stable EPs.

Example (cont.)

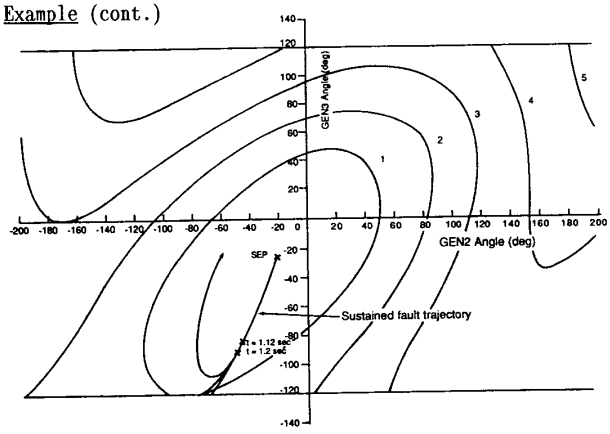

Fig. 3a: Potential Energy Surface, Point 'a'.

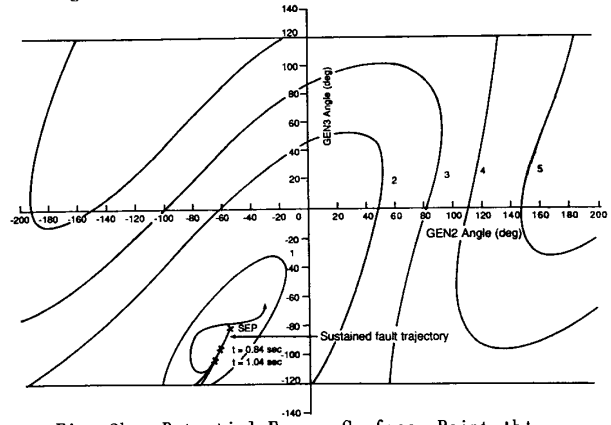

Fig. 3b: Potential Energy Surface, Point 'b'.

The impasse surface of this system can be found, using (A3) of Appendix A to be $|V_4|$=0.3873pu. By (4), that corresponds to α_3=±117.12°. Now, recall that the system of Fig. 1 has two stable (in terms of small disturbance analysis) EPs but no unstable EPs. By Theorem 2, those two points must be asymptotically stable so the system must have at least two PE sheets. They are shown in Figs. 3a and 3b. The potential energy of both figures is calculated relative to the stable EP 'a' of Fig. 2. This assists in imagining the sheets lying one above the other, pinched together at the impasse surface α_3=±117.12°.

Both PE sheets are locally positive definite. This agrees with the fact that the minimum energy points of both sheets are asymptotically stable. Figs. 3a and 3b confirm the fact that no unstable EPs exist for this power system. The impasse surface truncates the PE sheets before they fold over to form saddle points (unstable EPs). What are the consequences of this for large disturbance stability? We will come back to this point later. Over the PE sheet of Fig. 3a, all eigenvalues of $J_{\ell\ell}$ are positive. Over the other PE sheet, one eigenvalue of $J_{\ell\ell}$ is negative. The potential energy well is deeper in Fig. 3a than in Fig. 3b. This is consistent with the hypothesis that the stable EP of C_o has a larger stability margin than other stable EPs of the system. □

5.4 Large Disturbance Behaviour

Two types of behaviour can occur for disturbed systems modelled by SPM_o.

(i) Local behaviour within a set C_ℓ, i.e. the system remains on a single potential energy sheet. In Section 5.2 this behaviour was discussed for the case where C_ℓ contained a stable EP. If it does not contain a stable EP, stability must be lost either by angle separation or by loss of voltage causality. The type of unstable behaviour depends on the presence and location of unstable EPs.

(ii) Jumping between sets C_ℓ, i.e., from one sheet to another. Movement between sheets cannot occur smoothly. To do so, the system trajectory would have to pass through the impasse surface, which we have shown to be impossible. However, the system can jump between sheets upon step changes to system conditions, e.g. disturbance onset or clearing. The dynamics of the system during the step are in practice largely unknown and are not modelled in SPM_o. It is not possible therefore to predict whether a jump will occur, and if it does, to which sheet. Consequently stability assessment must assume the system remains on the same sheet during disturbances.

5.5 Consequences for a Stability Assessment Algorithm

Previous comments suggest that a stability assessment algorithm should be based on the usual concept of comparing attained energy with a critical value, V_{crit}. Determination of V_{crit} for SPM_o has some difficulties not previously encounted using traditional RNMs. A robust algorithm must be able to obtain an estimate for V_{crit} on any sheet, and in the presence of the impasse surface. Unstable EPs have played a vital role in determining V_{crit} in most algorithms to date. However the situation can now arise where a sheet contains a stable EP, but no unstable EPs (see the example).

Example (cont.)

We now return to our example of Fig. 1. This system was disturbed by the temporary loss of the feeder between GEN1 and BUS1. The effect of this disturbance is shown in Figs. 3a and 3b for initial conditions at points 'a' and 'b' of Fig. 2 respectively. Both these figures show the sustained fault trajectory, and system trajectories resulting when the disturbance was critically cleared, and cleared slightly later. Notice that in both cases critical clearing ensures stability. When cleared later, the system encounters the impasse surface, and voltage causality is lost.

Notice also that the critical clearing time is larger for the system with initial conditions at point 'a' than for the other case. This is consistent with the earlier remark that the lowest energy function sheet would have the largest stability margin. □

VI CONNECTIONS WITH VOLTAGE COLLAPSE

The concept of voltage causality (see Section 2.3) requires that load bus voltages behave in a predictable fashion, i.e., they follow the generator angles. However voltage causality says nothing about the voltages staying in a desired region around the normal operating point. The example of Fig. 1 is again a useful illustration. Fig. 4 shows the response of the voltage at BUS1 to the disturbance described in Section 5.5. When the disturbance was critically cleared, the voltage deviated quite dramatically, but was always dependent on generator angle movement. As the system settled to the stable EP the voltage returned to normal. That was not the case for delayed clearing. In that case the voltage fell to 0.3873pu, which coincided with the impasse surface, and voltage causality was lost. In this case the voltage certainly collapsed.

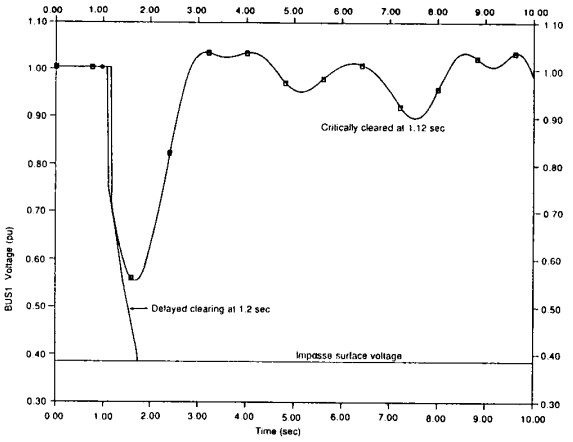

Fig. 4: Voltage Trajectories for Feeder Disturbance.

If all loads meet the conditions of Appendix A, voltage causality is ensured, except in the rare occasions when bus voltages fall to exactly zero. This does not mean that voltage excursions will be limited in any way during and after disturbances. It does however mean that if the system returns to a stable EP, voltages will settle to 'normal' values.

It remains to completely explore the connections to the bifurcation theory view of 'voltage collapse' [18, 19]. However, we note here that sudden reductions of voltage can occur simply as a consequence of system dynamics causing proximity to impasse surfaces. (The explanation in [18,19] gives significance to steady-state proximity to bifurcation points.) When the trajectory comes close to the impasse surface, jumps to different energy levels and lower voltages become likely.

VII CONCLUSIONS

This paper has explored the implications of using direct stability methods with power system models which include nonlinear loads. These so-called structure preserving models are a set of differential-algebraic equations. This introduces some new analytical issues over those encountered previously. These include multiple stable equilibria (which correspond to multi-sheeted energy surfaces) and voltage causality, with implications for voltage collapse behaviour in the network. Because of these difficulties, existing methods of determining and classifying equilibrium points are unsuitable. A new practical method is developed to achieve this. For a large class of load models, the analytical difficulties are not encountered. However, they must be considered for some realistic load conditions.

REFERENCES

[1] IEEE Committee Report, "Application of direct methods to transient stability analysis of power systems", *IEEE Trans. on Power Apparatus and Systems*, vol. PAS-103, No. 7, pp. 1629-1636, July 1984.

[2] A.A. Fouad, "Applications of transient energy functions to practical power system problems", *Symposium on "Rapid Analysis of Transient Stability"*, IEEE Power Engineering Society , Pub. no. 87TH0169-3-PWRS, 1987, pp. S-15.

[3] M.A. Pai, *Power System Stability*, North-Holland Pub. Co., New York, 1981.

[4] A.A. Fouad et al., "Direct transient stability analysis using energy functions application to large power networks", *IEEE Trans. on Power Systems*, vol. PWRS-2, No. 1, February 1987.

[5] R.M. Craven and M.R. Michel, "Load representation in the dynamic simulation of the Queensland power system", *Journal of Electrical and Electronics Engineering*, vol. 3, 1983, pp. 1-7.

[6] A.R. Bergen and D.J. Hill, "A structure preserving model for power system stability analysis", *IEEE Trans. on Power Apparatus and Systems*, vol. PAS-100, No.1, pp. 23-25, January 1981.

[7] P. Varaiya, F.F. Wu and R.L. Chen, "Direct methods for transient stability analysis of power systems: recent results", *Proc. of IEEE*, vol. 73, pp. 1703- 1715, December 1985.

[8] ESCA Corp., "Contribution to power system state estimation and transient stability analysis", Final Report to DOE, February 1984.

[9] N. Narasimhamurthi and M.T. Musavi, "A generalized energy function for transient stability analysis of power systems", *IEEE Trans. on Circuits and Systems*, vol. CAS-31, No.7, pp. 637-645, July 1984.

[10] N. Tsolas, A. Arapostathis and V. Varaiya, "A structure preserving energy function for power system transient stability analysis", *IEEE Trans. on Circuits and Systems*, vol. CAS-32, No. 10, pp. 1041-1049, October 1985.

[11] Th. Van Cutsem and M. Ribbens-Pavella, "Structure preserving direct methods for transient stability analysis of power systems", *Proc. 24th Conference on Decision and Control*, Ft. Lauderdale, Florida, December 1985.

[12] R.A. Schlueter, "A local potential energy boundary surface method for power system stability assessment", *Proc. 24th Conference on Decision and Control*, Ft. Lauderdale, Florida, December 1985.

[13] K.R. Padiyar and H.S.Y. Sastry, "Direct stability analysis of power systems with realistic generator models using topological energy functions", *IFAC Symposium on Power Systems and Power Plant Control*, Beijing, China, August 1986.

[14] C.N. Chong and D.J. Hill, "Energy function stability analysis of undamped power systems with nonlinear loads", *IEEE Trans. on Circuits and Systems*, to appear.

[15] D.J. Hill and C.N. Chong, "Lyapunov functions of Lur'e-Postnikov form for structure preserving models of power systems", *Automattca*, to appear.

[16] K.S. Chandrashekar and D.J. Hill, "A cutset stability criterion for power systems using a structure-preserving model", *Int. J. of Elec. Power and Energy Systems*, vol. 8, no. 3, pp. 146-157, July 1986.

[17] M. Lotfalian et al., "A stability assessment methodology", *IEEE Trans. on Power Systems*, vol. PWRS-1, no.2, pp. 84-91, May 1986.

[18] Y. Tamura, H. Mori and S. Iwamoto, "Relationship between voltage instability and multiple load flow solutions in electric power systems", *IEEE Trans. on Power Apparatus and Systems*, vol. PAS-102, no. 5, pp. 1115-1125, May 1983.

[19] H.G. Kwatny, A.K. Pasrija and L.Y. Bahar, "Static bifurcations in electric power networks: loss of steady-state stability and voltage collapse", *IEEE Trans. on Circuits and Systems*, vol. CAS-33, no. 10, pp. 981-991, October 1986.

[20] I.A. Hiskens and D.J. Hill, "Energy functions, transient stability and voltage behaviour in power systems with nonlinear loads", Technical Report EE8850, *Department of Electrical and Computer Engineering, University of Newcastle*, Australia, August 1988.

[21] C.L. De Marco and A.R. Bergen, "Application of singular perturbation techniques to power system transient stability analysis", Memo M84/7, *Electronics Research Laboratory, University of California*, Berkely, February 1984.

[22] D.J. Hill, "On the equilibria of power systems with nonlinear loads, *IEEE Trans. on Circuits and Systems*, to appear.

[23] S.-E. Mattson,"On differential/algebraic systems", Report TFRT-7327, *Dept. of Automatic Control, Lund Institute of Technology*, Sept.1986.

[24] W. Fleming, *Functions of Several Variables*, New York:Springer-Verlag, 1977.

[25] C. Concordia and S. Ihara, "Load representation in power system stability studies", *IEEE Trans. on Power Apparatus and Systems*, vol. PAS-101, no.4, pp. 969-977, April 1982.

[26] C.B. Price, "A generalized circle diagram approach for global analysis of transmission system performance", *IEEE Trans. on Power Apparatus and Systems*, vol. PAS-103, no. 10, pp. 2881-2, Oct. 1984.

[27] H. Yee and B.D. Spalding, "Transient stability analysis of multi-machine power systems by the method of hyperplanes", *IEEE Trans. on Power Apparatus and Systems*, vol. PAS-96, no.1, pp. 276-284, Jan. 1977.

[28] T. Athay, R. Podmore and S. Virmani, "A practical method for the direct analysis of transient stability", *IEEE Trans. on Power Apparatus and Systems*, vol. PAS-98, no.2, pp. 573-584, March 1979.

[29] L.O. Chua, "Dynamic nonlinear networks: state of the art", *IEEE Trans. of Circuits and Systems*, vol. CAS-27, no.11, pp. 1059-1087, November 1980.

APPENDIX A

Load Modelling to Ensure Voltage Causality

Let the voltage dependent loads be modelled as

$$P_{di} = P^0_{di}|V_i|^{p_i} \qquad i=1,\ldots,n_o \tag{A.1a}$$

$$Q_{di} = Q^0_{di}|V_i|^{q_i} \tag{A.1b}$$

instead of (2). Then it can be easily shown that

$$\frac{\partial f_{\ell i}}{\partial \alpha_i} = Q^0_{di}|V_i|^{q_i} - B_{ii}|V_i|^2 \tag{A.2a}$$

$$\frac{\partial f_{\ell i}}{\partial |V_i|} = P^0_{di}|V_i|^{p_i-1}(p_i-1) \tag{A.2b}$$

$$\frac{\partial g_i}{\partial \alpha_i} = -P^0_{di}|V_i|^{p_i-1} \tag{A.2c}$$

$$\frac{\partial g_i}{\partial |V_i|} = Q^0_{di}|V_i|^{q_i-2}(q_i-1) - B_{ii} \tag{A.2d}$$

Consider the case of a single load bus connected between two generator buses, as in Fig. 1. Then $\det \underline{J}_{\ell\ell}=0$ is equivalent to

$$(q_i-1)Q^2_{di} - q_iQ_{Bi}Q_{di} + Q^2_{Bi} + (p_i-1)P^2_{di} = 0 \tag{A.3}$$

where $Q_{Bi}=B_{ii}|V_i|^2$. Further manipulation yields

$$(Q_{di}+Q_{Bi})^2 + (q_i-2)(Q^2_{di}+Q_{di}Q_{Bi}) + (p_i-1)P^2_{di} = 0 \tag{A.4}$$

Voltage causality is ensured if no non-zero voltages satisfy (A.3) and (A.4). Load parameters which ensure this are found from (A.3),

$$p_i,\ q_i \geq 1 \tag{A.5a}$$

$$Q_{di}Q_{Bi} \leq 0 \tag{A.5b}$$

Further, from (A.4), it is obvious that if $q_i=2$, condition (A.5b) is not needed.

In [20], the analysis is extended to general load bus networks. It is shown that to ensure voltage causality:

i The admittance matrix of the load bus network must be negative definite. (This is the case in all practical power systems.)

ii $p_i \geq 1 \quad i=1,\ldots,n_o$

iii $q_i \simeq 2$ or $Q_{d_i} \simeq 0$, $i=1,\ldots,n_o$, i.e. either load power factor must be high, or the load must behave almost as constant admittance for voltage variations.

Discussion

R. Fischl, J-C Chow and **F. Mercede** (Drexel University, Philadelphia, PA): The authors are to be congratulated for introducing some new analytical issues which enable the establishment of a connection between the transient stability, multiple stable equilibria and voltage behavior. We have a few comments and questions and would appreciate the authors' response.

1. The example illustrates the theory for the case when Eq. (A.5a) is violated. It would be interesting to see what happens when Eq. (A.5a) is satisfied while Eq. (A.5b) is violated. Specifically, what will the results shown in Figs. 2 and 3 look like?
2. It is our understanding that the CONTUR program requires some value of a target function. What is the value of the target function used to plot the curve in Fig. 2? Moreover, can one obtain a similar curve when replacing the GEN2 MVAR by GEN2 $|V_g|$? If so, how does the 1-manifold change and can we use the same procedures to obtain the EP's?
3. It would be useful if the authors would show the relationship between the generator angle and voltage time history in Figure 4 for the two clearing times. Of particular interest is the voltage profile when the clearing time is 1.2 sec., which is the case when voltage causality is lost. Maybe by plotting both the generator angle and voltage profiles for this case, will give us a better understanding as to the difference between the angle stability and voltage stability.

In closing, we would like to complement the authors for an excellent paper.

Manuscript received February 27, 1989.

I. A. Hiskens and **D. J. Hill:** We wish to thank the discussors for their comments and questions. We shall answer the questions out of order.

Question 2

The traditional use of the CONTUR program involves the release of two system constraints and the introduction of one new constraint, namely the target function. A 1-manifold of course results as there is one more unknown then constraint. In our use of CONTUR for finding EPs, we have released the desired generator real power constraint plus any other system constraint. The target function then becomes that other system constraint. This results in a net reduction of one constraint, so a 1-manifold results.

This procedure allows generator real power to be plotted with reference to any function of state variables. GEN2 MVAr was chosen in Figure 2. Other choices could include generator angle, i.e., to produce a power-angle curve, or even system energy given by (13). GEN2 voltage would not be a useful choice as it is a fixed value.

Question 3

The relationship between generator angles and load bus voltages is governed by (4), i.e., the algebraic equations of the SPM_0 model. Because of the structure of the example system it is possible to obtain from those equations a simple relationship between GEN3 angle and BUS1 voltage of the form

$$h(\alpha_3, |V_4|) = 0$$

Notice that BUS1 voltage is dependent only on GEN3 angle, not GEN2 angle. The equation (14) is plotted in Figure 5.

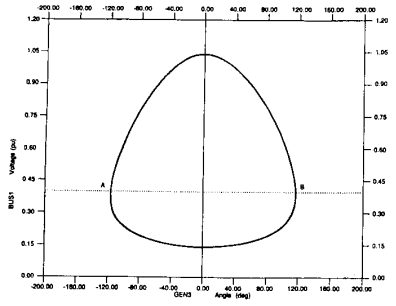

Fig. 5. Generator Angle/Bus Voltage Manifold-Constant Power Load.

This example illustrates a number of interesting concepts. As mentioned in the paper, the impasse surface is given by $\alpha_3 = \pm 117.12°$, i.e. points A and B in Figure 5. At these points the load bus voltage becomes infinitely sensitive to generator angle, i.e. a small change in angle results in a large change in voltage. This is characteristic of voltage collapse. Further, above the line AB J_{ll} has no negative eigenvalues, whilst below AB J_{ll} has one negative eigenvalue. Therefore, referring to Theorem 1, the curve between points A and B above line AB is the function ψ_0, whilst the curve below AB is ψ_1. This information is useful in interpreting the results of the disturbance of Section 5.5.

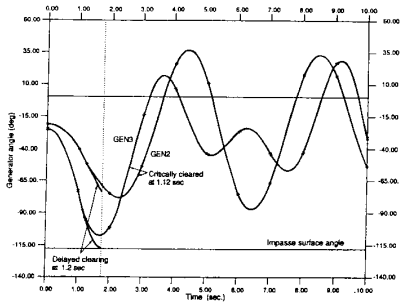

Fig. 6. Angle Trajectories for Feeder Disturbance.

The generator angle time responses for that disturbance are shown in Figure 6. When the disturbance was critically cleared, the impasse surface was not encountered, so the system trajectory remained within C_0. Therefore, the relationship between BUS1 voltage and the generator angles during the whole period was given by $|V_4| = \psi_0(\alpha_3)$. This is confirmed by comparing Figures 4, 5 and 6. Notice how sensitive BUS1 voltage is as GEN3 angle approaches the impasse surface. It is not surprising that the small increase in clearing time (to 1.2 seconds), which caused the angles to deviate just a little more, caused such a large voltage deviation.

In the delayed clearing case, point A of Figure 5 was encountered. Because of the singularity of J_{ll} at that point, the numerical integration technique failed.

Notice from Figure 3a that all points on the PEBS for the example system have high potential energy when compared with points along the impasse surface. It is therefore much more likely that the impasse surface, rather than the PEBS will be encountered by a disturbed system trajectory. Hence the most likely outcome of any disturbance of this system is loss of voltage causality. In general it is expected that the impasse surface and the PEBS will contain points of comparable potential energy. The ultimate form of instability, i.e. angle or voltage, will then depend on parameters such as disturbance type, location and length.

Question 1

Conditions (A.5) ensure global voltage causality. However, it is possible to find power systems where the conditions are not satisfied yet global voltage causality persists. This is particularly so with condition (A.5b).

To illustrate why (A.5b) can often be violated without J_{ll} becoming singular, consider the case of a load with indices of $p_i = q_i = 1$. Equation (A.3) becomes

$$Q_{B_i}^2 - Q_{B_i} Q_{di} = 0$$

Further manipulation yields the result that voltage causality is lost when

$$|V_i| = \frac{Q_{di}^0}{B_{ii}} \tag{15}$$

In normal situations the reactive load at a bus is small in comparison with the fault level, so this voltage is quite small. Such low voltages can seldom be achieved in realistic power systems, so voltage causality is not lost.

The example system of Figure 1 can be used to illustrate firstly that if (A.5b) is not satisfied then voltage causality is not ensured, and secondly that only under comparatively rare circumstances does (A.5b) become important.

Consider that system with a load at BUS1 of 50 − j30 MVA. If this load is modeled with voltage indices of $p = q = 1$, then from (15), voltage causality is lost when $|V_4| = 0.09$ pu. The plot of the algebraic equation (14) for this case, shown in Figure 7, does in fact indicate a breakdown in the voltage-angle relationship at $|V_4| = 0.09$ pu, i.e., points A and B. This situation is somewhat of a special case, as the location of the load bus

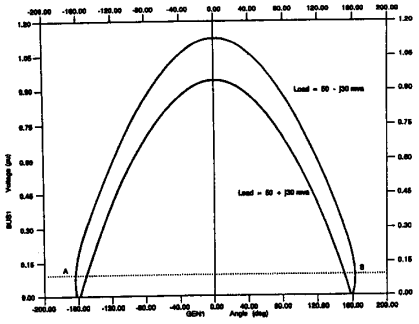

Fig. 7. Generator Angle/Bus Voltage Manifold-Load Indices p = q = 1.

midway between two generators allows the voltage to fall to such a low level. Note that because of this special situation, the voltage does in fact fall to zero.

Figure 7 also shows a plot of the algebraic equation when load was 50 + j30 MVA. As predicted by (A.3), the voltage sensitivity becomes infinite only when $|V_4| = 0.0$ pu.

In the capacitive load case, the GEN2 MW-MVAR plot was similar to Figure 2 up to the points where BUS1 voltage became zero. At those points the desired manifold intersects the manifold of constant zero voltage at BUS1, and CONTUR fails to converge. Also, the potential energy sheet for the "normal" stable EP is very similar to Figure 3a. The question of the form of the second potential energy sheet, i.e. whether it is similar to Figure 3b, has not been investigated. At such low voltages, i.e. less than 0.09 pu, the model is not a good representation of the power system.

In concluding, we wish to thank the discussers once more for their interest in our paper.

Manuscript received April 13, 1989.